Rare Metal Materials and Engineering
Volume 53, Issue 8, August 2024
Available online at www.rmme.ac.cn

Science Press

Cite this article as: Huang Junyuan, Zhang Wei, Fang Weiping, et al. Effect of Heat Treatments on Tribology Property of Ti6Al4V Alloy Under Dry Friction[J]. Rare Metal Materials and Engineering, 2024, 53(08): 2174-2181. DOI: 10.12442/j.issn.1002-185X.20230675.

ARTICLE

Effect of Heat Treatments on Tribology Property of Ti6Al4V Alloy Under Dry Friction

Huang Junyuan[1], Zhang Wei[1], Fang Weiping[2], Chen Jingyun[3]

[1] School of Mechanical Engineering & Automation, Beihang University, Beijing 100083, China; [2] China-Ukraine Institute of Welding, Guangdong Academy of Sciences, Guangzhou 510650, China; [3] Beijing Institute of Space Launch Technology, Beijing 100076, China

Abstract: Ti6Al4V alloy manufactured by electron powder bed fusion (EPBF) was separately heat-treated by stress-relief annealing at 600 °C, annealing at 800 °C, and solid solution at 920 °C for 1 h. Then, the friction and wear tests were conducted on the samples before and after heat treatment to analyze the properties and mechanism of friction and wear behavior. Results show that the sample annealed at 600 °C for 1 h has the optimal wear resistance, and the wear mass loss reduces by 44%. The sample annealed at 800 °C for 1 h possesses the optimal anti-friction performance, and the coefficient of friction reduces by 14%. This research provides a simple heat treatment method to improve the friction and wear resistance of Ti6Al4V alloy manufactured by EPBF.

Key words: Ti6Al4V alloy; electron powder bed fusion; heat treatment; anti-friction performance; wear resistance

Titanium alloys have been widely used in biomedicine, military energy, automobile industry, aerospace, and petrochemical fields due to their excellent performance and low cost[1–2]. Ti6Al4V alloy has good plasticity and strong corrosion resistance, which is mainly used in the aircraft compressor discs and blades, large-size forgings, and die forgings[3–4]. Electron powder bed fusion (EPBF) has the advantages of fast processing and high productivity[5]. In recent years, the preparation of Ti6Al4V alloy by EPBF process has been widely researched[6–7].

Titanium alloys have disadvantages, such as poor plastic shear resistance, low protective effect of surface oxides, and inferior friction and wear properties[8–9]. Through modification treatment and surface strengthening, the microstructure of Ti6Al4V alloy can be ameliorated to improve the friction and wear properties[10–11]. Sasaki et al[12] found that compared with that of EPBFed Ti6Al4V alloy, the erosion rate of EPBFed Ti6Al4V alloy after heat treatment was decreased by approximately 40% and 95% due to cavitation peening and abrasive cavitation peening, respectively. Chen et al[13] prepared ceramic coatings on Ti6Al4V alloy surface by micro-arc oxidation. When the addition of hexagonal boron nitride was 1.5 g/L, the friction coefficient of the coating was the smallest. Adhesive wear is accompanied by slight abrasive wear. Salguero et al[14] replaced conventional Ti6Al4V alloy surfaces with textured surfaces and reduced the friction by 62% and wear by two orders of magnitude. Li et al[15] investigated the friction and wear behavior of Ti6Al4V alloy after cryogenic treatment under low load (5 N), low scratch speed (5 cm/s), and dry/wet conditions, and found that the cryogenic treatment improved the hardness, enhancing the friction and wear properties of titanium alloy.

Heat treatment can change the internal structure of the material and eliminate various defects in the thermal processing process, thereby improving the performance and prolonging the service life of the parts[16–17]. Compared with other improvement methods, heat treatment has the advantages of simplicity, no pollution, and easy control, and it is often used to improve the performance of Ti6Al4V alloy[18–19]. Zhou et al[20] reported that the three-stage heat treatment could simultaneously improve the yield strength, ultimate tensile strength, and elongation of laser melting-deposited Ti6Al4V alloy. Wang et al[21] found that the Ti6Al4V alloy after low-temperature heat treatment exhibited a slightly improved strength and the enhanced elongation with increment of 26%, resulting in a combination of high strength

Received date: October 29, 2023
Foundation item: National Natural Science Foundation of China (51975036); Guangdong Province Key R&D Project (2018B090904004)
Corresponding author: Zhang Wei, Ph. D., Professor, School of Mechanical Engineering & Automation, Beihang University, Beijing 100191, P. R. China, E-mail: zhangweibh@buaa.edu.cn

and good ductility. Ju et al[22] investigated the effect of heat treatment at 760 – 1060 °C on the tribological behavior of selective laser-melted Ti6Al4V alloy against Si_3N_4 counter-ball under different applied loads. It was found that the wear rate of as-built Ti6Al4V alloy is increased firstly and then decreased with the increase in heat treatment temperature. However, the effect of heat treatment on the tribological properties of Ti6Al4V alloy manufactured by EPBF has rarely been studied[23–24].

In this research, the electron beam additive was used to manufacture Ti6Al4V alloy, and different heat treatment methods were used to analyze and compare the friction coefficient and wear rate of Ti6Al4V alloy after heat treatment. Through surface morphology and composition measurements, the friction and wear mechanisms of different samples were analyzed to achieve suitable heat treatment for further improvement in the anti-friction and wear resistance of Ti6Al4V alloy manufactured by EPBF.

1 Experiment

The additive manufacturing samples were prepared by EPBF additive manufacturing equipment, which was jointly developed by Beihang University and the Aviation Industry Manufacturing Technology Research Institute. Ti6Al4V alloy powder was provided by AVIC Matt Additive Technology (Beijing, China) Co., Ltd. Ti6Al4V alloy was processed through EPBF. During EPBF processing, the power was 500 W, the line spacing and layer spacing were both 0.1 mm, and the scanning speed was 1 m/s.

The additively manufactured samples were heat-treated at various temperatures using muffle furnace (SG-QF1400, Shanghai Sager Furnace Co., Ltd, China). The samples without heat treatment were used as control group and denoted as U. The samples subjected to stress-relief annealing were denoted as HT600: they were put into muffle furnace, heated at 600 °C for 1 h, and then cooled in the furnace[25]. The samples subjected to annealing at 800 °C for 1 h were denoted as HT800[26]. The samples subjected to solid solution treatment (heating in the furnace at 920 °C for 1 h and then water cooling) were denoted as HT920[27]. By the wire electric discharge machine (MV series, Mitsubishi, Japan), the prepared samples were cut into the ones of 10 mm×10 mm×2 mm. The small samples were polished with sandpaper (500#, 1000#, 2000#).

Ti6Al4V alloy is often used to manufacture bearing frames, which usually suffers spherical-surface friction with bearing balls, and the sizes and specifications of bearing frames are different[28]. Therefore, the linear reciprocation friction form was used to simulate the working conditions of infinite bearing frames. A reciprocation friction tester (SRV5, Optimol, German) was used. The friction test temperature was 22 °C, and the humidity was 24%. Si_3N_4 ceramic has the characteristics of high strength, high acid and alkali resistance, and high wear resistance, which can reduce the influence of wear products on the friction and wear behavior of titanium alloy materials. Thus, Si_3N_4 ceramic ball counterpart was used in this research[29]. The diameter of Si_3N_4 ceramic balls (Yast Company, China) was 4 mm, and the hardness HV was 13 720 – 16 660 MPa[30–31]. The experiment was conducted with the small load sensor (10 N) to prevent the worn out phenomenon. The loading force was 5 N, the speed was 10 mm/s, the stroke was 5 mm, and the friction test duration was 30 min. Each experiment was repeated 3 times.

Scanning electron microscope (SEM, MIRA LMS, TESCAN, Czech Republic) was used to observe the surface morphology of the samples, and the energy dispersive X-ray spectrometer (EDS) was used to detect the surface composition. The three-dimensional topography and wear volume of the wear scar surface were measured using the white light interferometer (Q8 MAGELLAN, Bruker, Germany). Abrasion mass was measured using a balance (Meilen, China). Surface chemical bonds and chemical composition were characterized using X-ray photoelectron spectroscopy (XPS, ESCALAB 250Xi, Thermo Scientific, USA). The crystals were characterized using the electron backscattered diffractometer (EBSD, Hikari Plus, EDAX, USA). The Channel 5 software was used to analyze EBSD data.

2 Results and Discussion

2.1 Friction coefficient and wear rate

Fig. 1a illustrates the coefficient of friction (COF) curves of U, HT600, HT800, and HT920 samples. Fig. 1b displays the average COF and error of the samples. It can be seen that COF decreases firstly and then increases after different heat treatments, and the COF of all heat-treated samples is less than 0.517. The COF order of different samples is as follows: $COF_U > COF_{HT600} > COF_{HT920} > COF_{HT800}$. Compared with that of U

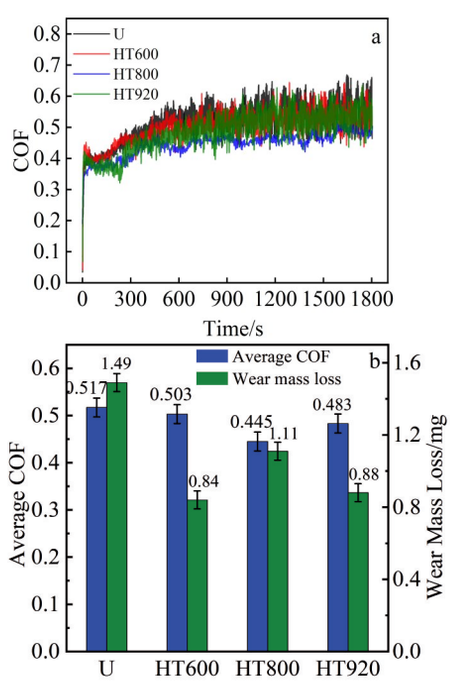

Fig.1 COF curves (a) and average COF values with wear mass loss (b) of U, HT600, HT800, and HT920 samples

sample, the COF of HT600, HT800, and HT920 samples reduces by 3%, 14%, and 7%, respectively. HT800 sample has the lowest COF value of 0.445.

Fig.1b also shows the wear mass loss of U, HT600, HT800, and HT920 samples. The wear mass loss of the heat-treated samples is smaller than that of the unheated-treated U sample. The wear mass loss of Si_3N_4 ceramic balls is consistent with that of the corresponding samples. The wear mass loss of Si_3N_4 ceramic balls is shown in Table 1[32]. The order of mass wear rate of different samples is $M_U > M_{HT800} > M_{HT920} > M_{HT600}$. Compared with that of U sample, the mass wear rate of HT600, HT800, and HT920 samples decreases by 44%, 26%, and 41%, respectively.

2.2 Surface morphology

SEM surface morphologies and 3D wear scares of different samples are shown in Fig.2. Before tribology tests, the surface is smooth. Afterwards, obvious adhesive wear marks and abrasive wear marks can be observed[33]. According to Fig.2b–2c, the surface adhesion and abrasive wear marks are the most serious, which is manifested as adhesive wear and abrasive wear. Fig. 2f – 2g show that the adhesion marks of HT600 sample are less than those of U sample, presenting weaker adhesive wear and abrasive wear. Fig.2j–2k show that HT800 sample mainly has adhesive wear marks with a small number of abrasive wear marks, but the adhesion degree is slighter than that of other samples. In general, the degree of adhesive wear and abrasive wear of HT800 sample is slighter than that of other samples[34–35]. Fig.2n–2o show that HT920 sample has obvious adhesive wear scars and abrasive wear scars, and its wear degree is similar to that of HT600 sample, presenting weaker adhesive wear and abrasive wear. According to the 3D wear scare morphologies of different samples, the wear scar depth of U, HT600, and HT920 samples are close to 24 μm, whereas that of HT800 sample is about 18 μm. Therefore, the wear degree of HT800 sample is the slightest[36], which is consistent with SEM observation conclusions.

Table 1 Wear mass loss of Si_3N_4 ceramic balls during tests of U, HT600, HT800, and HT920 samples (mg)

Sample	Wear mass loss
U	0.05±0.005
HT600	0.02±0.005
HT800	0.04±0.005
HT920	0.03±0.005

The wear mass loss of Si_3N_4 ceramic balls is extremely small and the ceramic ball surfaces are smooth, resulting in the fact that the wear marks are not visible to the naked eyes due to reflection, as shown in Fig.3. Therefore, the position of the wear scar cannot be determined, the morphology of the wear scar cannot be observed, and the subsequent measurements cannot be continued. Thus, only the

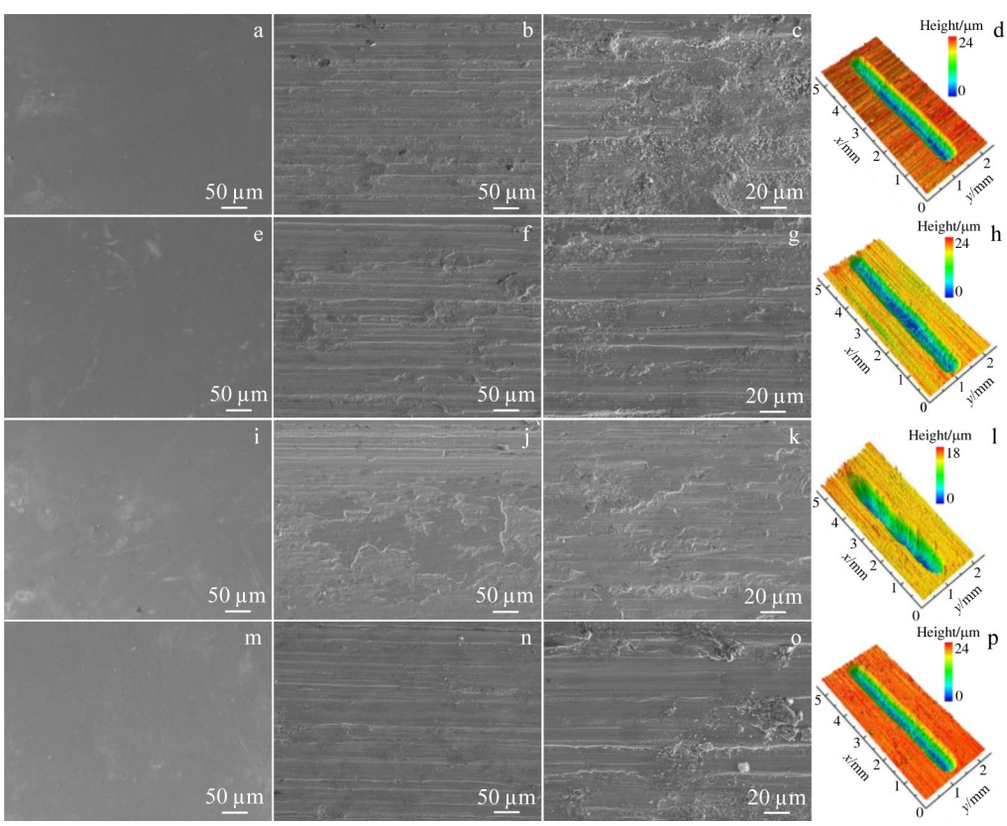

Fig.2 SEM surface morphologies of U sample (a–c), HT600 sample (e–g), HT800 sample (i–k), and HT920 sample (m–o) before (a, e, i, m) and after (b–c, f–g, j–k, n–o) wear tests; 3D wear scare morphologies of U sample (d), HT600 sample (h), HT800 sample (l), and HT920 sample (p)

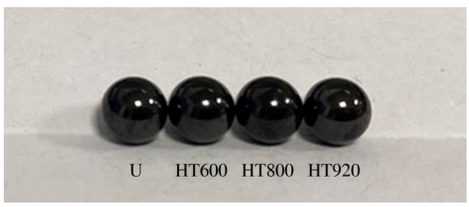

Fig.3 Appearance of Si_3N_4 ceramic balls after tribology test

tribological behavior of Ti6Al4V alloy manufactured by EPBF was discussed.

SEM crystal phase morphologies of U, HT600, HT800, and HT920 samples are shown in Fig. 4. It can be seen that the microstructure is composed of elongated α grains and intergranular β grains. With the increase in heat treatment temperature, the width and spacing of β grains are increased, and the size of α grains is also increased gradually. The

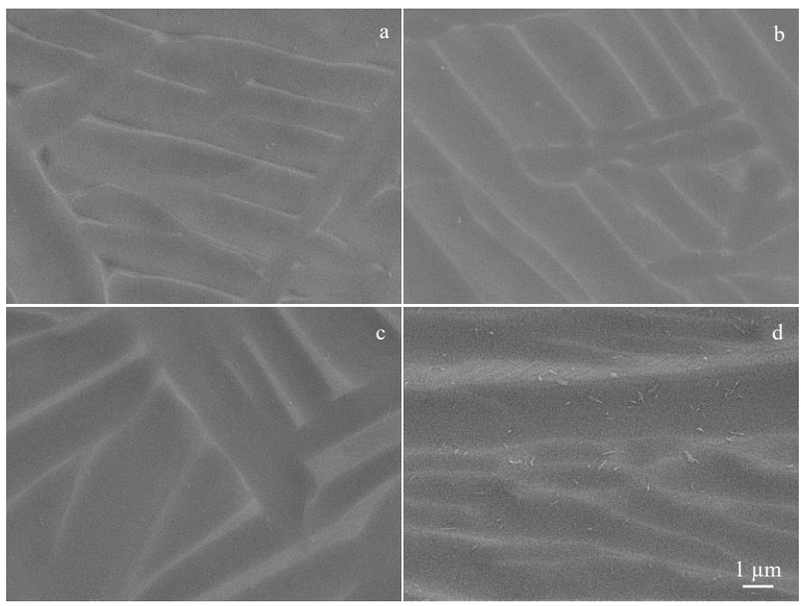

Fig.4 SEM crystal phase morphologies of U sample (a), HT600 sample (b), HT800 sample (c), and HT920 sample (d)

proportion of the hard α phase and soft β phase in the sample was measured, as shown in Fig. 5. The proportion of the β phase decreases firstly, then increases, and finally decreases, which is consistent with the variation of wear rate. The higher the proportion of β phase, the smaller the sample microhardness, the easier the plastic deformation, and the greater the wear rate. HT800 sample has the highest proportion of β phase. These results indicate that HT600 sample has the optimal wear resistance. However, HT800 has the optimal anti-friction performance: its COF reduces by

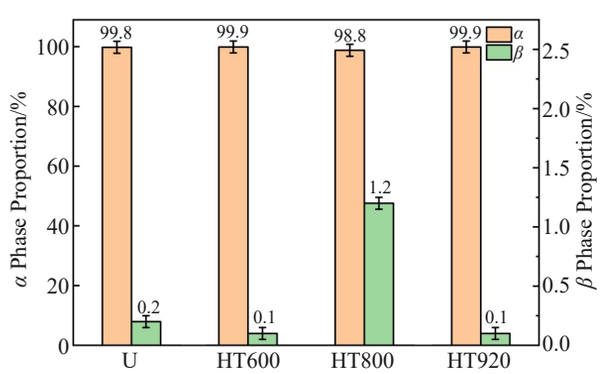

Fig.5 Proportion of α and β phases in U, HT600, HT800, and HT920 samples

14%, the wear mechanism is abrasive, adhesive, and corrosive wear, but the wear degree is the slightest.

2.3 Surface composition

The surface element content differences of U, HT600, HT800, and HT920 samples before and after tribology tests are shown in Table 2. After tribology tests, the contents of C, O, and Si elements on the surface increase, and the contents of Al, Ti, and V elements decrease. After tribology tests, the contents of N and Si elements in U, HT600, and HT920 samples all increase, indicating that there are obvious Si_3N_4 residues[37]. However, the N element content of HT800 sample

Table 2 EDS surface element content difference of U, HT600, HT800, and HT920 samples before and after tribology tests (±0.5at%)

Element	U	HT600	HT800	HT920
C	2.09	1.36	3.39	4.28
N	5.82	5.86	0.00	2.76
O	15.34	10.17	34.44	14.82
Al	−2.47	−1.85	−4.79	−2.17
Ti	−20.26	−15.14	−41.07	−19.27
V	−0.87	−0.69	−1.27	−0.94
Fe	−0.04	−0.02	8.83	0.04
Si	0.41	0.32	0.46	0.47

barely changes. Additionally, there is still a small amount of Si element, indicating that Si_3N_4 remains on the surface. Still, corrosion and wear may occur, resulting in changes in the original N element content on the surface[38]. At the same time, the content of O element in HT800 sample increases obviously by 34.44at%. It is believed that the severe oxidation occurs, i. e., corrosion wear occurs[39]. The content of Fe element in U, HT600, and HT920 samples barely changes, but that in HT800 sample increases by 8.83at%, which further proves that the HT800 sample has obvious corrosive wear during friction[40].

The chemical bonds in the samples were detected to further confirm the friction and wear mechanisms. As shown in Fig.6, after tribology tests, the intensity of Si element on the surface is not obvious, and no peaks of other elements appear[41–42]. Fig. 7 shows XPS spectra of different elements. For better comparison efficiency, XPS spectra of samples before and after tribology tests are presented in the same diagram. In

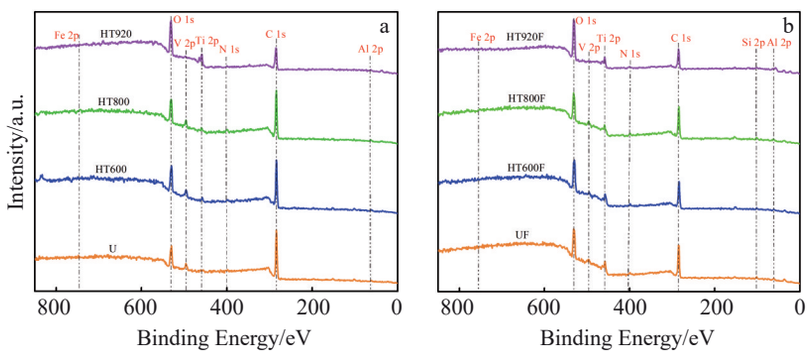

Fig.6 XPS spectra of U, HT600, HT800, and HT920 samples before (a) and after (b) tribology tests

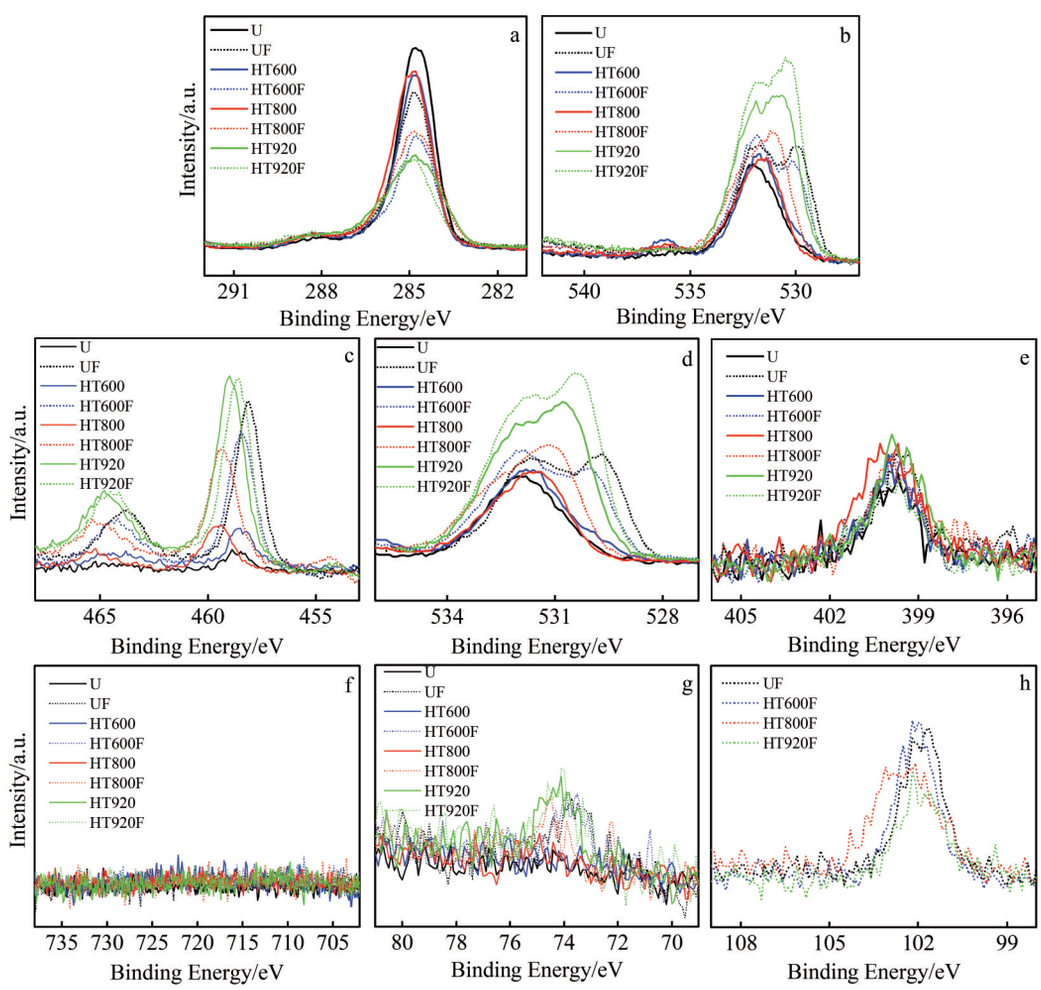

Fig.7 XPS spectra of C (a), O (b), Ti (c), V (d), N (e), Fe (f), Al (g), and Si (h) elements in U, HT600, HT800, and HT920 samples before and after tribology tests

Table 3 XPS surface element content difference of U, HT600, HT800, and HT920 samples before and after tribology tests (±0.5at%)

Sample	C	N	O	Al	Ti	V	Fe	Si
U	−19.16	0.67	9.24	0.76	5.14	0.04	0.53	2.78
HT600	−17.97	0.81	8.93	0.74	4.8	−0.16	−0.47	3.31
HT800	−14.42	0.13	7.47	0.38	3.25	−0.18	0.21	3.16
HT920	−8.78	−0.75	5.6	−0.04	−0.81	−0.06	2.69	2.13

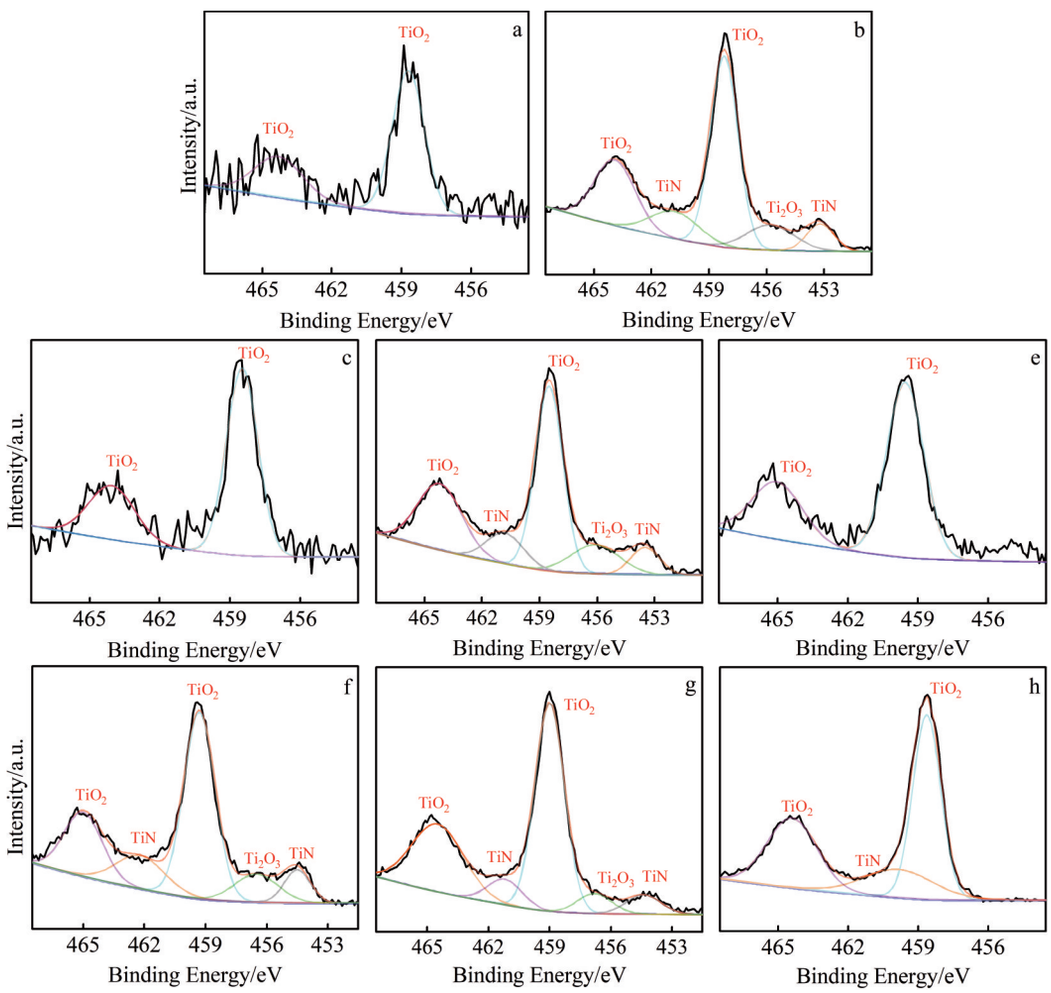

Fig.8 XPS spectra of Ti element in U (a), UF (b), HT600 (c), HT600F (d), HT800 (e), HT800F (f), HT920 (g), and HT920F (h) samples

order to distinguish the samples, the samples after tribology tests are labeled with F in the sample name. Compared with the samples before friction, the peak intensity of C element after friction becomes significantly lower, and the other peak intensities also vary from high to low. The peak of Si element appears after tribology tests. Table 3 shows XPS surface element content difference of U, HT600, HT800, and HT920 samples before and after tribology tests. It can be seen that the C content significantly reduces, and the contents of O and Si elements increase.

XPS spectra of Ti element are shown in Fig. 8. It can be seen that U, HT600, and HT800 samples only have TiO_2 before tribology tests. After friction, Ti_2O_3 and TiN are formed in U, HT600, and HT800 samples[43]. In U, HT600, and HT800 samples, Ti_2O_3 and TiN appear. After tribology tests of HT920, only TiO_2 and TiN are left on the surface. The content and error of the surface Ti components are shown in Fig. 9.

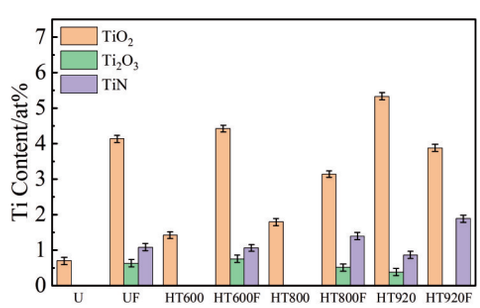

Fig.9 Ti component contents in U, HT600, HT800, and HT920 samples before and after tribology tests

The TiO_2 contents in U, HT600, and HT800 samples all increase after tribology tests, whereas those of HT920 sample decrease. It is considered that oxidation corrosion wear occurs in the friction process of U, HT600, and HT800 samples[44–45].

In summary, through surface composition and surface phase analyses, it is found that the higher the surface O content of the heat-treated sample, the smaller the COF value; the higher the β phase content, the greater the wear rate.

3 Conclusions

1) Abrasive wear, adhesive wear, and corrosive wear occur in U sample, and its COF and wear rate are the largest.

2) The wear resistance of HT600 sample is optimal, and the mass wear rate reduces by 44%.

3) HT800 sample has the optimal anti-friction performance: its COF reduces by 14%, whose wear mechanism is abrasive, adhesive, and corrosive wear, and the wear degree is the slightest.

4) The degree of adhesive wear and abrasive wear of HT920 sample is similar to that of HT600 sample. No corrosive wear can be detected in the HT920 sample, and the solid solution treatment has a certain reduction effect on the friction and wear.

5) Heat treatment can reduce the COF and wear rate of Ti6Al4V alloy manufactured by EPBF. The tribological properties of Ti6Al4V alloy manufactured by EPBF can be improved simply through heat treatment without pollution. This research provides a reference for the performance enhancement of additive manufacturing.

References

1 Pushp P, Dasharath S M, Arati C. *Materials Today: Proceedings*[J], 2022, 54: 537

2 Arif Z U, Khalid M Y, Al Rashid A *et al*. *Optics & Laser Technology*[J], 2022, 145: 107447

3 Pan X L, Wang X D, Tian Z *et al*. *Journal of Alloys and Compounds*[J], 2021, 850: 156672

4 Yin L W, Umezawa O. *International Journal of Fatigue*[J], 2022, 156: 106688

5 Lv N, Liu D, Hu Y *et al*. *Engineering Failure Analysis*[J], 2022, 137: 106269

6 Terrazas C A, Murr L E, Bermudez D *et al*. *Journal of Materials Science & Technology*[J], 2019, 35(2): 309

7 Zhang W, Tong M, Harrison N M. *Additive Manufacturing*[J], 2019, 28: 610

8 Yang Junwei, Tang Haibo, Tian Xiangjun *et al*. *Rare Metal Materials and Engineering*[J], 2023, 52(9): 3316 (in Chinese)

9 Jin X Y, Lan L, Gao S *et al*. *Materials Science and Engineering A*[J], 2020, 780: 139199

10 Sahoo S, Chou K. *Additive Manufacturing*[J], 2016, 9: 14

11 Wu Yanquan, Zhou Jun, Zhang Chunbo *et al*. *Rare Metal Materials and Engineering*[J], 2023, 52(9): 3132 (in Chinese)

12 Sasaki H, Take F, Soyama H. *Wear*[J], 2020, 462: 203518

13 Chen X W, Ren P, Zhang D *et al*. *Surface Innovations*[J], 2022, 11(1–3): 49

14 Salguero J, Del S I, Vazquez-Martinez J M *et al*. *Wear*[J], 2019, 426: 1272

15 Li Y G, Wang X F, Yang S Q *et al*. *Materials*[J], 2019, 12(18): 2850

16 Qin M, Zhang L M, Zhao X R *et al*. *Advanced Science*[J], 2021, 8(8): 2004640

17 Nezhadfar P D, Shrestha R, Phan N *et al*. *International Journal of Fatigue*[J], 2019, 124: 188

18 Waqas M, He D Y, Liu Y D *et al*. *Journal of Materials Engineering and Performance*[J], 2023, 32(2): 680

19 Zou Z, Simonelli M, Katrib J *et al*. *Materials Science and Engineering A*[J], 2021, 814: 141271

20 Zhou Y, Wang K, Sun Z G *et al*. *Journal of Materials Processing Technology*[J], 2022, 306: 117607

21 Wang Q P, Kong J, Liu X K *et al*. *Vacuum*[J], 2021, 193: 110554

22 Ju J, Zhao C L, Kang M D *et al*. *Tribology International*[J], 2021, 159: 106996

23 Buhairi M A, Foudzi F M, Jamhari F I *et al*. *Progress in Additive Manufacturing*[J], 2023, 8(2): 265

24 Davoodi E, Montazerian H, Mirhakimi A S *et al*. *Bioactive Materials*[J], 2022, 15: 214

25 Li J Q, Lin X, Wang J *et al*. *Corrosion Science*[J], 2019, 153: 314

26 Peng C, Liu Y, Liu H *et al*. *Journal of Materials Science & Technology*[J], 2019, 35(10): 2121

27 Liu G T, Leng K, He X H *et al*. *Progress in Natural Science: Materials International*[J], 2022, 32(4): 424

28 Ji H C, Peng Z S, Huang X M *et al*. *Journal of Materials Engineering and Performance*[J], 2021, 30(11): 8257

29 Yu D L, Zhu Z X, Min J L *et al*. *Advances in Applied Ceramics*[J], 2021, 120(1): 47

30 Huang J Y, Cai L M, Zhang W *et al*. *Tribology International*[J], 2022, 174: 107747

31 Sadeghi M, Kharaziha M, Salimijazi H *et al*. *Surface and Coatings Technology*[J], 2019, 362: 282

32 Zambrano O A, Muñoz E C, Rodríguez S A *et al*. *Wear*[J], 2020, 452: 203298

33 Li J H, Ren W B, Ren Y Z *et al*. *Optical Engineering*[J], 2023, 62(1): 015102

34 Huang J Y, Zhang W. *Rare Metal Materials and Engineering*[J], 2024, 53(2): 357

35 Jamil M, He N, Zhao W *et al*. *Tribology International*[J], 2021, 156: 106812

36 Zhou Z Y, Liu X B, Zhuang S G *et al*. *Applied Surface Science*[J], 2019, 481: 209

37 Shankar S, Nithyaprakash R, Santhosh B R *et al*. *Tribology International*[J], 2020, 151: 106529

38 Zhang D Y, Du X, Bai A *et al*. *Wear*[J], 2022, 510–511: 204494

39 Asl H G. *Vacuum*[J], 2020, 180: 109578

40 Brończyk A, Kowalewski P, Samoraj M. *Wear*[J], 2019, 434:

202966
41 Zhang D, Cui X F, Jin G *et al*. *Tribology Transactions*[J], 2019, 62(5): 779
42 Hua S W, Pang M, Ji F Q *et al*. *Materials Today Communications*[J], 2023, 34: 105165
43 Wang Y, Zhang M, Li K *et al*. *Optics & Laser Technology*[J], 2021, 139: 106987
44 Yao R, Yao Z P, Li Y *et al*. *Surface and Coatings Technology*[J], 2023, 454: 129152
45 Abe J O, Popoola A P I, Popoola O M. *Materials Science and Engineering A*[J], 2020, 774: 138920

热处理对干摩擦 Ti6Al4V 合金摩擦性能的影响

黄俊媛[1]，张　伟[1]，房卫萍[2]，陈静云[3]
(1. 北京航空航天大学 机械工程及自动化学院，北京 100191)
(2. 广东省科学院 中乌焊接研究所，广东 广州 510650)
(3. 北京航天发射技术研究所，北京 100076)

摘　要：对电子粉床熔合（EPBF）制造的Ti6Al4V合金分别进行1 h的600 ℃去应力退火、800 ℃退火和920 ℃固溶热处理，然后对热处理前后的试样进行摩擦磨损实验，分析比较摩擦磨损性能和机理。结果表明，600 ℃去应力退火+1 h热处理后的试样耐磨性能最佳，磨损质量减少了44%。800 ℃退火+1 h热处理后的试样减摩性能最好，摩擦系数减小了14%。本研究提供了一种简单的热处理方式，提高了EPBF制造Ti6Al4V合金的减摩耐磨性能。

关键词：Ti6Al4V合金；电子粉床熔合；热处理；减摩性能；耐磨性能

作者简介：黄俊媛，女，1993年生，博士生，北京航空航天大学机械工程及自动化学院，北京 100191，E-mail：jyhuang@buaa.edu.cn